SUBSEA PIPELINE WALKING: THE EFFECT OF A BI-LINEAR SEABED FRICTION MODEL

Indranil Guha, PhD Candidate, University of Western Australia**,** Australia,guhanil@gmail.com
David J. White, Professor of Infrastructure Geotechnics**,** University of Southampton, Southampton, UK**,** david.white@soton.ac.uk
Mark F Randolph, Professor, Fugro Chair in Geotechnics, Centre for Offshore Foundation Systems, University of Western Australia, Australia, mark.randolph@uwa.edu.au

ABSTRACT

The objective of this paper is to explore the gaps in the present analysis methods proposed by various joint industry projects and others for pipeline walking behaviour. Thereafter, present analytical methods are extended to bridge the gap between analytical modelling tools and numerical analysis, by extending analytical models to encompass bi-linear soil friction behaviour. In the analytical solution, the pipe-soil interaction is usually modelled as rigid-plastic, expressed as ultimate resistance per unit length. Often this term is expressed non-dimensionally as a friction factor, μ. However, the elastic-plastic (i.e. bi-linear) behaviour of the soil and the effect of this bi-linear response of the soil on the walking behaviour were not addressed in the literature. The elastic-plastic behaviour is often represented by an additional parameter, specified as the mobilisation displacement. This is defined as the amount of axial displacement that occurs before the ultimate friction is generated, and the resistance rises linearly with displacement up to this value. The walking behaviour is affected by the axial friction mobilisation displacement. The existing analytical solutions are extended to incorporate the elastic-plastic response of the soil into the expression of pipeline walking, supported by a new derivation. Numerical verification with ABAQUS is also provided for the proposed expression.

INTRODUCTION

The increasing demand for energy is not only pushing the hydrocarbon industry towards the deeper oceans but also pushing the operating conditions towards the high temperature and high pressure (HT/HP) regime. Therefore, the present deepwater submarine pipelines are being operated at HT/HP which can require special design considerations to prevent issues related to thermal expansion, such as buckling and walking. Theories of buckling have been developed in the last two decades and are well accepted in the industry. (e.g., DNV RP-110; Collberg et al. 2011). The so-called pipeline walking mechanism was also well defined in last few years by various researches (Konuk, 1998, Tørnes et. al. 2000) and by the industry projects such as SAFEBUCK JIP (Carr et. al. 2006, Collberg et al 2011). However, understanding the walking mechanism is becoming challenging with the increasing complexities related to soil-pipe interaction on soft clays, particularly when considering detailed aspects of pipe-soil interaction behaviour.

Once the pipeline is laid on the seabed, it is heated or cools down during operation cycles. Due to this heat up and cool down process the pipe tends to expand and contract respectively. These expansion and contractions are resisted by the seabed friction. When it cools down the pipe cannot regain the original unstressed configuration due to the seabed resistance. This phenomenon is addressed in pipeline design guidelines. In some cases the pipeline expansion leads to a global displacement of the pipe because the expansion and contraction are asymmetric between the two ends, leading to a net movement of the pipe in one direction. This is commonly known as 'walking' of pipeline. Walking itself is not a limit state, but uncontrolled walking may lead to many of the critical problems, such as, overstressing of end connectors such as spool pieces and jumpers, loss of tension in a SCR (Steel catenary riser), increased loading within a lateral buckle and route curve pull-out of the restrained system (Carr et. al. 2006). Carr et al (2006) gave the expressions for the pipeline walking under various field conditions in work that was part of the SAFEBUCK JIP. They expressed that, the pipeline walking behaviour of short pipelines can occur due to (1) tension at the end of pipelines, associated with a steel catenary riser (SCR), (2) global seabed slope along the length of the pipe, and (3) thermal gradients along the pipeline during changes in operating conditions. Bruton et al. (2010) added a fourth mechanism, being (4) changes in the distribution of weight

along the pipeline due to liquid hold upon shutdown. In this paper walking due to the first three mechanisms were considered for the analysis and further study. The walking due to slope with liquid hold up could be studied separately based on the proposed model as a further study. In the following section existing pipeline walking mechanisms for various seabed slopes, SCR tensions and thermal transients have been examined with numerical solutions. However, the elastic-plastic response of the soil was neglected at this stage. To incorporate the mobilisation displacement of the soil into the existing methodology to predict walking of submarine pipelines, a new analytical solution is developed later in this paper.

NUMERICAL ANALYSIS OF WALKING – VERIFICATION OF EXISTING THEORIES

Numerical analysis is described in this section to reproduce the existing theories and to give an insight into the existing practiced methodologies to estimate pipeline walking rates without recourse to numerical analysis. As mentioned earlier, walking due to SCR tension, seabed slope and thermal transients have been studied and, numerical results are compared with the existing theories for validation of the numerical modelling. Finite element analysis (FEA) was performed with commercial software ABAQUS (Dassault Systèms, 2011) Ver. 6.11.2. The pipeline was modelled with pipe (PIPE31) elements and the seabed was modelled with analytical rigid elements available in the ABAQUS code. The friction between the pipeline and seabed was modelled with friction force being proportional to the normal force. The static method was used in ABAQUS to simulate the heating of the pipeline uniformly. Table 1 shows the material properties used for the pipeline.

Table 1: Input data used for comparison analysis

Material properties:	**Parameters**	**Units**
Diameter, D	0.912	m
Wall thickness, t	0.033	m
Length, L	2000	m
Young's modulus, E	210	GPa
Unit weight of the pipe, W'	6.902	kN/m
Poisson's ratio, ν	0.3	
Coefficient of thermal expansion, α	12 x E-06	/ ° C
Temperature rise, $\Delta\theta$	90	° C
Friction factor, μ	0.1 ~ 0.6	
SCR tension, T_{SCR}	100~500	kN
Seabed slope, φ	0 ~ 3	° (angle)
Thermal gradient, q_θ	10 ~ 30	°C/km

Following idealisations are made to carry out the FEA:

- The pipeline remains elastic and the material properties are described by Young's modulus E, Poisson's ratio υ, linear expansion coefficient α; since the transient response is not considered the thermal conductivity and specific heat are not relevant.
- The pipe can be treated as a straight thin-walled circular tube of thickness t and the mean radius R (defined as ½ (outer diameter – t)).
- The pipeline is empty and there is no internal pressure acting inside the pipeline
- The temperature of the pipeline is considered uniform for the present analysis. However, the actual temperature profile is complicated. The actual temperature profile was often assumed in the literature to decay exponentially with distance from the hot end.
- The left end of the pipe was considered to be fixed on the well or at a manifold or termination structure and the right end was considered to the free for expansion. This assumption was similar to the analysis of half-length of the pipe with both ends free.

The pipeline is assumed to be connected to the wellhead and can expand freely away from the wellhead. The wellhead is at a very high temperature. When the high-temperature oil or gas starts flowing through the pipeline it is subjected to a temperature gradient $\Delta\theta$, which results in a tendency to expand away towards the free end. Over the length L, the pipeline moves away from the wellhead, and so the bottom exerts on the pipe a force f, per unit length, directed towards the wellhead and opposing the motion. Due to the restriction of movement, a compressive load P develops in the pipeline.

Walking due to SCR tension

Existing analytical models are compared here with the numerical results. Input parameters are as tabulated in Table 1. Figure 1 shows comparisons of analytical and numerical results for two different friction factors, μ = 0.1, 0.6. The walking rate is examined for a range of SCR tensions. The walk per cycle, Δ_{SCR} is inversely proportional to the friction factor and directly proportional to the SCR tension, keeping other parameters remain constant. These numerical results are in good agreement with the existing analytical solution (Carr et. al. 2006).

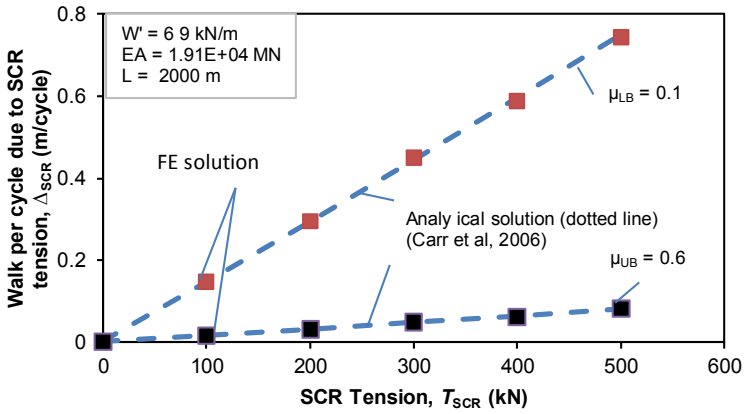

Figure 1: Comparison of analytical and FE solutions for walking with SCR tension

Walking due to Seabed slope

The walk per cycle calculated analytically using the method described by Carr et. al. (2006) has been compared with the numerical results. Input parameters were tabulated in Table 1. Figure 2 shows a comparison of analytical and numerical results for two different friction factors, μ = 0.1, 0.6. The walking rate is examined for a range of seabed slopes (φ = 0°- 3°). The walk per cycle, Δ_{φ} is inversely proportional to the friction factor and directly proportional to the seabed slope, keeping other parameters constant. The present numerical results are in good agreement with the existing analytical solution (Carr et. al. 2006).

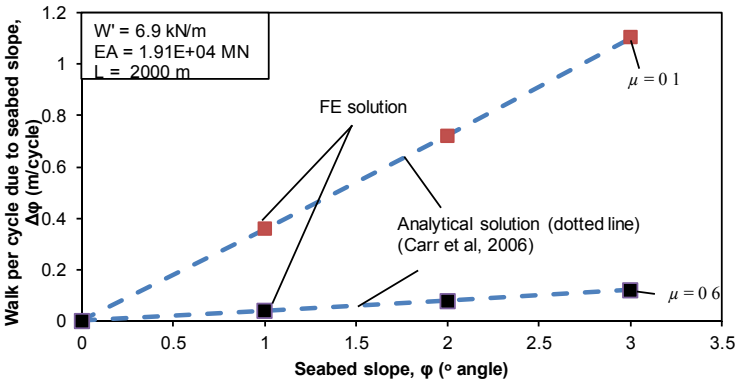

Figure 2: Comparison of analytical and FE solutions for walking with a sloping seabed

Walking due to Thermal transients

The thermal gradient applied to a pipeline has a significant effect on the walking rate. Figure 3 illustrates the walking rate, Δ_T as a function of the axial friction force normalised by the constraint friction, f^*. For a pipeline to be fully mobilised during operating condition (loading and unloading) the change in fully constraint force (ΔP) should be more than the axial frictional resistance, $F_{passive}$. Therefore, the constraint friction at which the cyclic constraint occurs, f^* is defined as $f^* = \Delta P / L$ (Carr et. al. 2006). Three different thermal gradients were used to compare the walking rate between existing analytical expression (Carr et. al. 2006) and the present numerical solution. The results of the numerical analysis and the analytical

solution match with good agreement. The amount of walking is strongly influenced by the thermal gradient, i.e. the walking rate of 30°C/km is 3 times that of 10°C/km for the same *f*/*f**.

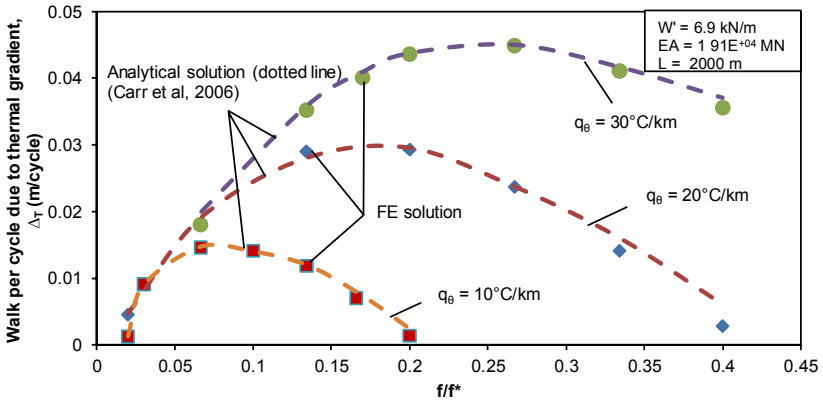

Figure 3: Comparison of analytical and FE solutions for pipeline walking with thermal transients

EFFECT OF BI-LINEAR FRICTION ON WALKING

Having verified that the numerical analysis is performed in this work is accurate, through comparison with existing analytical solutions for pipeline walking, the numerical analysis was extended to an elastic-plastic axial friction model. The amount of pipeline walking is also influenced by the mobilisation displacement of the axial friction model. A bi-linear axial response was used in FE analysis, with the mobilisation displacement being the displacement required to mobilise the full axial resistance. The effect of mobilisation displacement on the walking behaviour of the pipelines has been discussed by various authors (Tørnes et. al. 2000, Carr et. al. 2006,) and explored numerically and more recently analytically (Wang et. al. 2010). For example, Wang et al. (2010) explored the effect of mobilisation displacement on long pipelines and a 'caterpillar-type' locomotion was discussed. An analytical model for the effect of mobilisation displacement on the walking of short pipelines is developed in the present paper. This section gives a detailed insight into this behaviour and thereafter provides an expression to estimate the walking rate for elastic-plastic axial friction.

Approach

Firstly, numerical analysis was carried out to see the effect of mobilisation displacement on the walking. Different mobilisation displacements with the same ultimate friction were used to compare the results. The force profiles were also compared. Thereafter, an analytical model was developed to analyse the effect of mobilisation displacement on the force profile and hence on the walking. The next two short sections give the details of numerical and analytical modelling to investigate the effect of mobilisation displacement on the walking behaviour of submarine short pipelines.

Numerical analysis

Details of the numerical analysis to investigate the effect of mobilisation displacement on the walking behaviour of submarine pipelines resting on a seabed slope and subjected to thermal cycles are described in this section. Three different mobilisation displacements, u_{ult}, of 0.001 m, 0.05 m, and 0.1 m were considered and are shown in Figure 4. An elastic perfectly plastic Coulomb friction model was chosen as discussed earlier. The pipe material, size and length were kept constant as earlier cases. The seabed was considered with a slope of, φ = 3°, and a minimum friction factor of 0.1 was considered to recover larger end expansions, minimising the influence of numerical errors.

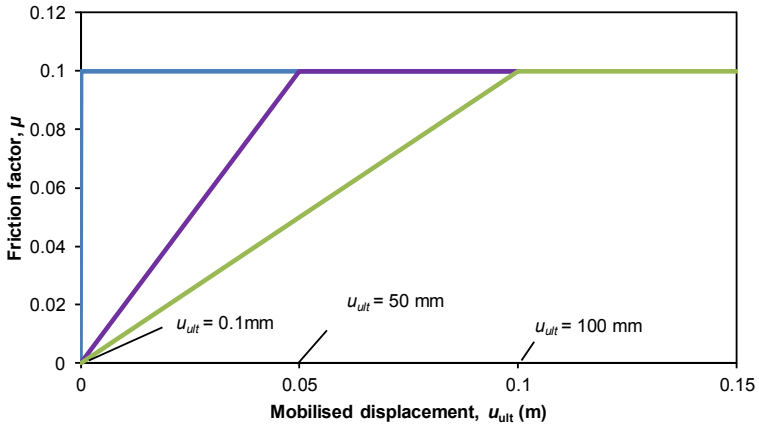

Figure 4: Mobilisation displacements and elastic-plastic friction models considered in this paper

The expansion at the downslope end of the pipe, δ is plotted against cycle number for different mobilisation displacements in Figure 5. The effect of mobilisation displacement becomes prominent after the first two cycles.

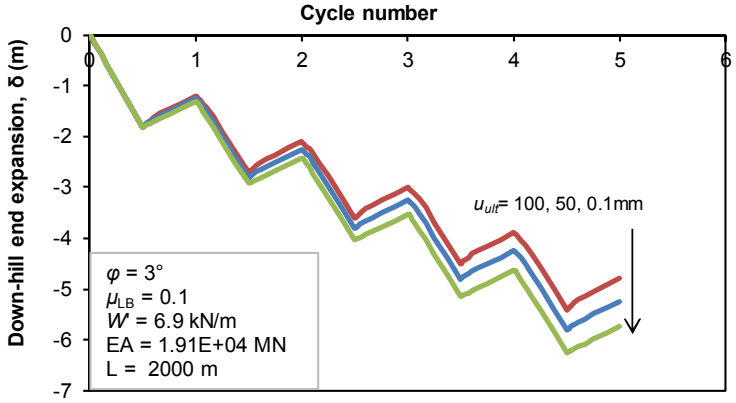

Figure 5: Effect of mobilisation displacement on a pipeline with the sloping seabed and minimum friction

Figure 6 shows how the mobilisation displacement affects the walking of a pipeline on a sloping seabed. This shows that with increasing mobilisation displacement, the walking rate reduces. The walking rate of the pipeline for various seabed slopes is also plotted for different mobilisation displacements.

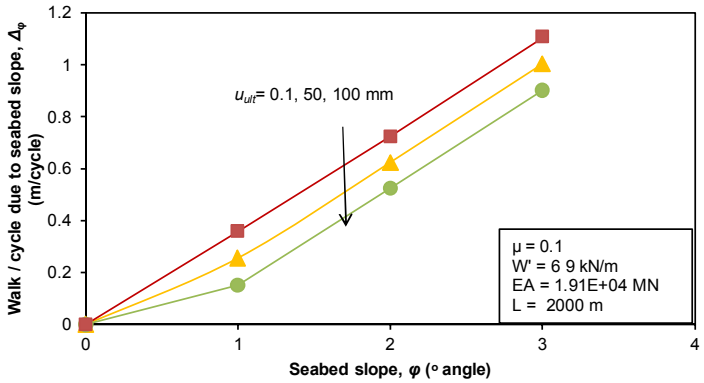

Figure 6: A summary of the effect of mobilisation displacement on the walking rate

To investigate the effect of mobilisation displacement on the walking behaviour of the pipeline, the force profiles during heat up and cool down steps are plotted for various mobilisation displacements, u_{ult} = 0.001, 0.1, 0.2, 0.3, & 0.456 m, with seabed slope, φ = 3°, and friction of 0.1 for the same pipe considered previously (0.456 m = 0.5*D*). Figure 7 shows the force envelopes of the pipeline for heat up and cool down steps from very low to very high mobilisation displacement. The virtual anchor points show a very sharp edge with u_{ult} = 0.001 m, and the crown of the force envelops became parabolic with increasing u_{ult}. The sharper peak is due to the full mobilization of the friction along the length of the pipeline. The phenomenon is explained analytically in the following section.

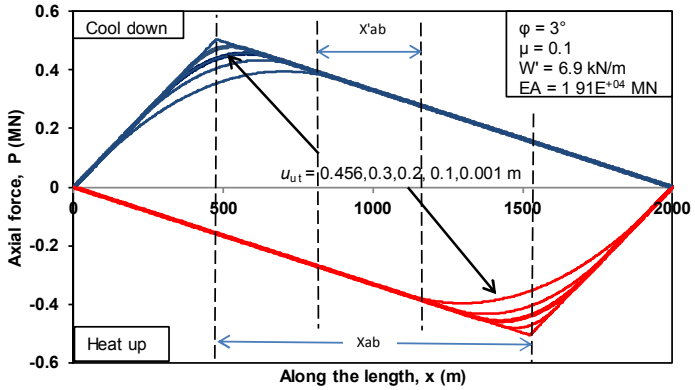

Figure 7: Comparing force profiles for various mobilisation displacements

Analytical solution

Figure 8 shows the resulting force profile of a pipeline with, *EA* = 19 GN, *L* = 2000 m, φ = 3°, u_{ult} = 0.456 m, $\Delta\theta$ = 90°C. Only the cool-down step is plotted here. Only half of the force envelope is considered, as this is a symmetrical case. The force profile has been divided into four parts and the force profile for these four parts is derived to compare the analytical and numerical results.

From elasticity theory:

$$\frac{du}{dx} = \frac{P}{EA} \tag{1}$$

Therefore, with axial frictiona resistance, $F_{passive}$, axial displacement, *u* and axial pipe-soil stiffness, *k*, the equilibrium equation can be expressed as

$$\frac{dP}{dx} = F_{passive} = uk = u\left(\frac{\mu W}{u_{ult}}\right) \tag{2}$$

Differentiating equation (1) and using equation (2) gives

$$\frac{d^2P}{dx^2} = P\left(\frac{\mu W}{EAu_{ult}}\right) = \lambda^2 P \tag{3}$$

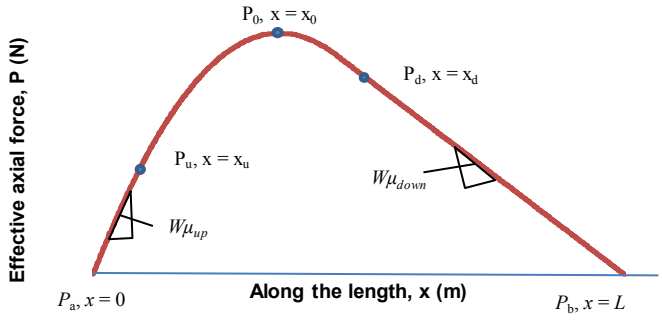

Figure 8: Force profile after unloading stage for a finite mobilisation displacement

where, $\lambda^2 = \left(\frac{\mu W}{EAu_{ult}}\right)$, noting that λ takes two values, λ_{up} and λ_{down}. The general solution of the equation is given by

$$P(x) = Ae^{\lambda x} + Be^{-\lambda x} \tag{4}$$

The slopes of the uphill and downhill force profile are given by

$$\frac{dP_{up}(x)}{dx} = \lambda_{up}\left(A_{up}e^{\lambda_{up}x} - B_{up}e^{-\lambda_{up}x}\right) \tag{5}$$

and

$$\frac{dP_{down}(x)}{dx} = \lambda_{down}\left(A_{down}e^{\lambda_{down}x} - B_{down}e^{-\lambda_{down}x}\right) \tag{6}$$

Again, the relationship between x_m and L can be expressed as

$$\frac{x_m}{L - x_m} = \frac{\mu_{down}}{\mu_{up}} \tag{7}$$

and the distance between two unloading virtual anchor points, x_d and x_m by

$$x_d - x_m = \frac{u_{ult}EA}{\left(\Delta P - \Delta S_f\right)} \tag{8}$$

where, $\Delta S_f = \mu_{down}WL$, the length of the unloading virtual anchor point without mobilisation displacement is x_m, and the length of the unloading virtual anchor point with mobilisation displacement is x_d.
Using various boundary conditions and solving the equations we get

$$A_{down} = \frac{\mu_{down}W}{\lambda_{down}} \frac{1}{\left[e^{\lambda_{down}x_u} - e^{\lambda_{down}(2x_0 - x_d)}\right]} \tag{9}$$

and, $$B_{down} = \frac{\mu_{down}W}{\lambda_{down}} \frac{e^{2\lambda_{down}x_d}}{\left[e^{\lambda_{down}x_u - e^{\lambda_{down}(2x_0 - x_d)}}\right]} \tag{10}$$

Again, it can be shown (see Figure 8) that the new anchor length, X'_{ab} is linked to the previous anchor length X_{ab} by

$$X'_{ab} = X_{ab} - 2(x_d - x_m) \tag{11}$$

Therefore, the new walk per cycle is given by

$$\Delta_{ult} = \frac{\left(\Delta P - \Delta S_f\right)X'_{ab}}{EA} \tag{12}$$

Using equation (11), we get

$$\Delta_{ult} = \frac{\left(\Delta P - \Delta S_f\right)X_{ab}}{EA} - \frac{\left(\Delta P - \Delta S_f\right)}{EA} \cdot \frac{2u_{ult}EA}{\left(\Delta P - \Delta S_f\right)} \tag{13}$$

Therefore, the ultimate walking per cycle for the elastic-plastic friction model is given by

$$\Delta_{ult} = \Delta_{\varphi} - 2u_{ult} \tag{14}$$

The first term in the left-hand side is the walk per cycle due to a slope for a rigid plastic seabed (i.e. without a mobilisation displacement) and the second term is double the mobilisation displacement. The same soil elastic stiffness was used for loading and unloading cases, meaning that an increase of u_{ult} in the mobilisation displacement reduced the walk by $2u_{ult}$ per cycle. The above expression can be used to predict the walking of submarine pipelines, taking into account the recoverable elastic component of the mobilisation displacement. Further cases were analysed to explore how the mobilisation displacement affects the walking of pipeline triggered by SCR tension and thermal transient.

ESTIMATING PIPELINE WALKING WITH ELASTIC-PLASTIC SEABED FRICTION

Numerical modelling was carried out to analyse the walking affected by the mobilisation displacement for SCR tension and thermal transients, in addition to the case of seabed slope that is analysed above. Analytical and numerical results were then compared to verify the exactness of the proposed model when applied to both the slope case (derived above) and also the other cases. All three walking mechanisms were studied here. The material properties of the pipe and the heating range were kept constant as given in Table 1. The results in all cases showed that the correction by $2u_{ult}$ of the rigid-plastic solution gives the correct walking rate for the elastic-plastic friction model. Therefore, the solution that is proven analytically above for the seabed slope case is also applicable to the thermal transient and SCR cases.

Effect of mobilisation displacement on SCR tension triggered pipeline walking

Figure 9 illustrates the comparison between predicted and numerical results of the walk per cycle. The mobilisation displacements were varied from 0.001 m to 0.456 m (0.5D) to investigate the validity of the model. Predicted and numerical results match with good agreement for the case of SCR tension.

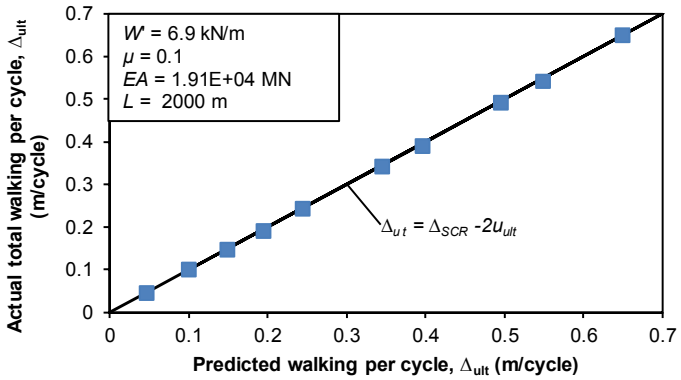

Figure 9: Verifying the effect of mobilisation displacement on walk per cycle due to SCR tension

Effect of mobilisation displacement on seabed slope triggered pipeline walking

Figure 10 shows the comparison between predicted and numerical results of the walk per cycle. The mobilisation displacements were varied from 0.001 m to 0.456 m (0.5*D*) to investigate the validity of the model. Predicted and numerical results match with good agreement for the case of seabed slope.

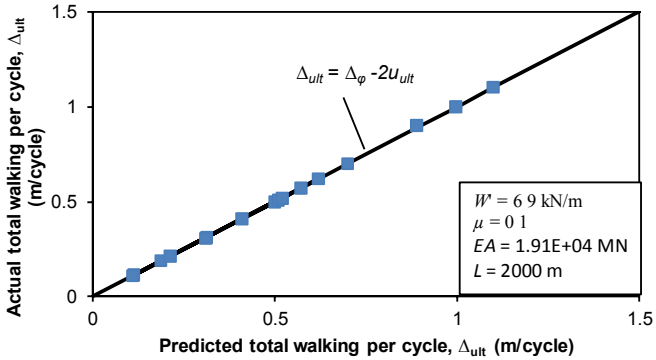

Figure 10: Verifying the effect of mobilisation displacement on walk per cycle due to seabed slope

Effect of mobilisation displacement on thermal transients triggered pipeline walking

Figure 11 shows the comparison between predicted and numerical results of the walk per cycle. The mobilisation displacements were varied from 0.001 m to 0.456 m (0.5*D*) to investigate the validity of the model. Predicted and numerical results match with good agreement for the case of thermal transients.

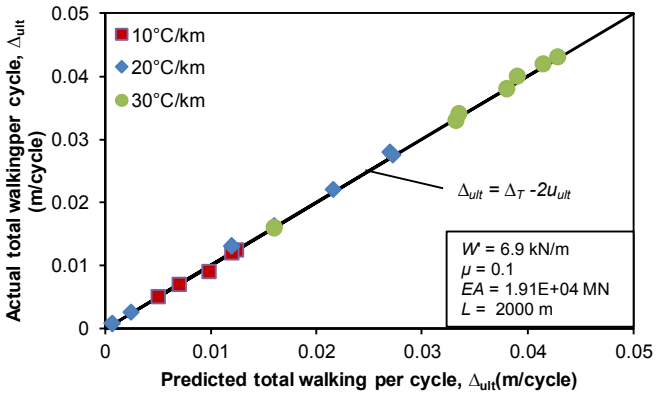

Figure 11: Verifying the effect of mobilisation displacement on walk per cycle due to thermal transients

Design Chart

A simple design chart is shown in Figure 12, illustrating how to estimate the walking rate of a pipeline on a seabed slope of 3º with friction factors, μ = 0.1 to 0.6, keeping all other parameters the same as above. Points A and B (0.9 and 08 m) are the walking rates for mobilisation displacements of 100 and 150 mm respectively.

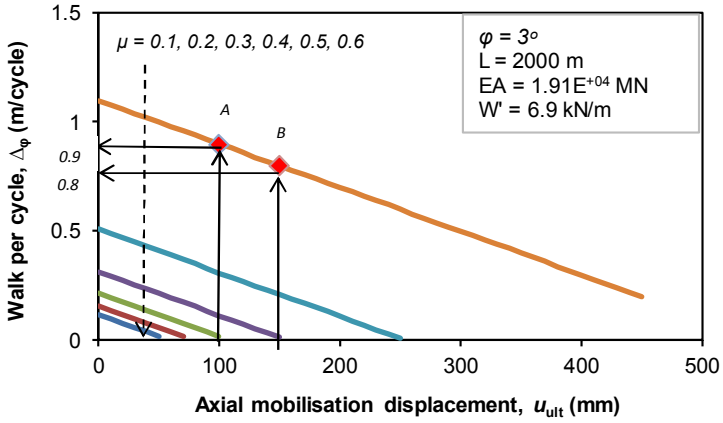

Figure 12: Illustration of the effect of mobilisation displacement on the walking rate for a 3° seabed slope

CONCLUSIONS

This paper bridges the gap between the present analytical design tool for pipeline walking towards a more realistic soil response. The existing analytical methods to predict pipeline walking has been used to verify a numerical model and an analytical solution has been developed to incorporate the elastic-plastic response into the existing solution for walking down a sloping seabed. The solution was also shown to apply to walk due to SCR tension and thermal transients based on full numerical analysis. A new expression was therefore proposed to predict the walking rate on elastic-plastic soil response. This is proven analytically for the slope case and shown numerically to apply for other cases, as a modification of the rigid-plastic solutions.

ACKNOWLEDGEMENT

This work forms part of the activities of the Centre for Offshore Foundation Systems (COFS), established in 1997 under the Australian Research Council's Special Research Centres Program, and supported (2010-2017) as a node of the Australian Research Council's Centre of Excellence for Geotechnical Science and Engineering, and through the Fugro Chair in Geotechnics, the Lloyd's Register Foundation Chair and Centre of Excellence in Offshore Foundations and the Shell EMI Chair in Offshore Engineering.

REFERENCES

Brunner, M. S., Qi, X., Zheng, J., & Chao, J. C. 2006. Combined effect of flowline walking and riser dynamic load on HP/HT flowline design. Proc. of Offshore Technology Conference, Houston, USA, OTC 17806.

Bruton, D., Sinclair, F., & Carr, M. 2010. Lessons learned from observed walking of pipelines with lateral buckles, including new driving mechanisms and updated analysis models. Proc. of Offshore Technology Conference, Houston, USA, OTC 20750

Bruton, D., White, D. J., Carr, M., & Cheuk, J. C.Y. 2008. Pipe-soil interaction during lateral buckling and pipeline walking-The SAFEBUCK JIP. Proc. of Offshore Technology Conference, Houston, USA, OTC 19589.

Carr, M., Bruton, D., & Leslie, D. 2003. Lateral buckling and pipeline walking, a challenge for hot pipelines, Offshore Pipeline Technology Conference. Amsterdam.

Carr, M., Sinclair, F., & Bruton, D. 2006. Pipeline Walking – Understanding the filed layout challenges, and analytical solutions developed for the SAFEBUCK JIP. Proc. of Offshore Technology Conference, Houston, USA, OTC 17945

Chaudhury, G., 2010. Managing unidirectional movements (walk) of HPHT submarine flowlines during startup heating and shutdown cooling. Proc. of 5th International Offshore Pipeline Forum, ASME, Houston, USA. ISOPE 2010-1003

Collberg, L., Carr, M. and Levold, E. (2011). Safebuck Design Guideline and DNV-RP-F110. Proceedings of the Offshore Technology Conference. OTC21575, Houston, USA. DOI: 10.4043/21575-MS.

Dassault Systèmes (2007) Abaqus analysis user's manual, Providence, RI.

DNV-RP-F110, DNV Recommended Practice F110 "Global Buckling of Submarine Pipelines – Structural Design due to High Temperature/High Pressure" Det Norske Veritas, Norway October 2007 (free to download from www.dnv.com)

Hill, A. J., & Jacob, H. (2008). In-situ measurement of pipe-soil interaction in deep water. Proc. of Offshore Technology Conference, Houston, USA, OTC 19528.

Konuk, I., 1998. Expansion of pipelines under cyclic operational conditions: Formulation of problem and development of solution algorithm. Proc of 17th International Conference on Offshore Mechanics and Arctic Engineering. OMAE98-1103

Rong, H., Inglis, R., Bell, G., Huang, Z., & Chan, R. (2009). Evaluation and mitigation of axial walking with a focus on deep water flowlines. Proc. of Offshore Technology Conference, Houston, USA, OTC 19862.

SAFEBUCK JIP – Safe Design of Pipelines with Lateral Buckling, Design Guideline, SAFEBUCK II, 2008. (Confidential to participants)

Tørnes, K., Ose, B.A., Jury, J., Thomson, P. 2000. Axial Creeping of High Temperature Pipelines caused by Soil Ratcheting. Proc. of 19th Int. Offshore Mech. and Arctic Eng.LA, USA. OMAE2000/PIPE-5055

Wang, Y. N., Maschner, E. A., & Hayes, R. (2010). A global migration risk to partially constrained long pipelines subjected to localized thermal gradient cycles. Proc of the 29th International Conference on Ocean, Offshore and Arctic Engineering, ASME, Shanghai, China, OMAE2010-20784.